We appreciate thoughtful reading and constrictive comments provided by the reviewer. We also thank for taking time and providing all the minor comments. Thanks to these corrections the paper is significantly improved now, as we believe. Below please find our point-to-point replies. The responses to the reviewer comments are given in blue text; the original reviewer comments are in black text.

Anonymous Referee #2

Received and published: 14 January 2016

This paper presented a computational tool to calculate the direct aerosol radiative effect by accounting for the detailed spectral and angular scattering properties of aerosol and surface reflectance. Using this tool, they evaluated the instantaneous and diurnally averaged radiative efficiencies of five aerosol models over different surface types. Furthermore, they carried out sensitivity tests on how different treatment of surface reflectance, aerosol particle shape, and aerosol phase function affect the instantaneous and diurnal averaged aerosol radiative effect.

I found the large positive radiative forcing over the northern Sahara surprising. As shown in Fig. 7, the daily averaged aerosol radiative efficiencies at the top of the atmosphere is about 15 Wm-2tau-1 for a mixture of dust and biomass burning aerosols when surface albedo is about 0.3. As indicated in Fig. 13, the TOA radiative effect reaches to about 20 Wm-2 in central Egypt, where the AOT is about 0.2 to 0.3, the surface albedo is about 0.3, and the SSA (440 nm) is about 0.88. This indicates that the aerosol type responsible for this large positive radiative effect has a radiative efficiency 3 to 4 times larger than the dust and biomass burning mixture presented in Fig. 7. In the western and northern part of Western Sahara, the direct aerosol radiative effect also reaches to about 15 Wm-2, where the AOT is about 0.5, the surface albedo is about 0.3, and the SSA (440 nm) is about 0.88. I would think this case closely resemble the dust aerosol model presented in Fig. 7, which always has a negative radiative efficiency. Can you explain why your calculated radiative effect is positive? Authors indicated that the low SSA and high albedo cases encounter in the northern Africa was not included in their theoretical calculations, I would suggest that authors extend their calculation to include these high albedo and low SSA cases to support the very large positive aerosol radiative effect obtained in Fig. 13.

We absolutely agree with the reviewer's suggestion to extend the calculations for high surface albedo and low SSA cases to support results obtained in Fig. 13 of the discussion version of the manuscript. Results of the complementary calculations do support the obtained values and are presented in a new figure. We also explain reasons of high radiative efficiency that is correctly figured out by the reviewer. We therefore considerably extended Section 8 titled "Illustration of radiative effect calculations over Africa". In the end of this document we present an extended version of Section 8 with two additional figures and updated Fig. 13 (Fig. 14 in the new version, it also includes now the maps of aerosol radiative efficiency).

There are quite a few AERONET sites in northern Africa. I would suggest the authors to compare their POLDER/PARASOL retrieved AOT/SSA with the AERONET retrievals. I understand there will be some differences due to temporal and spatial mismatches, nonetheless the comparison will still be helpful.

A comparison of AOT and SSA retrieved by GRASP from POLDER/PARASOL with

AERONET is included now in the updated Section 8. Please see below the new version of Section 8.

Minor comments:

Page 6, line 29, typo “incudes”.
Corrected.

Page 6, line 30, should be “a set of”.
Corrected.

Page 6, line 31, what is the spectral resolution used for the aerosol complex refractive index.
It is explained in the same section, several sentences later on as the next:
The aerosol optical thickness, Single Scattering Albedo (ω_0), and phase function ($P(\Theta)$) (or phase matrix) are calculated for each of 208 spectral intervals using the size distribution, complex refractive index and fraction of spherical particles. The missing spectral values of the complex refractive index are linearly interpolated or extrapolated from the values provided in the input since spectral behaviors of aerosol complex refractive index in the solar spectrum is sufficiently smooth.

Page 7, line 1, what parameters are used for the aerosol vertical distribution?
This is the vertical profile of aerosol extinction. The sentence is clarified as follows:
It should be noted that in the presented studies the vertical distribution of aerosol extinction was fixed and assumed as a Gaussian distribution with maxima at an altitude of 1 km and standard deviation of 0.7.

Page 7, line 3, typo “In”, should be “It”.
Corrected.

Page 8, line 24, should be “one of these advancements”.
Corrected.

Page 9, line 1, I think it reads better if you structure your sentence like this “the radiative effect calculation strategy described above is”.
Thank you, the sentence is modified as follows:
The radiative effect calculation strategy described above is therefore driven by this motivation and is tied to the retrieved characteristics provided by GRASP.

Page 10, line 31-32, I am surprised that only Angstrom exponent is used to classify dust aerosols, why not also using fraction of non-spherical particles?
Thank you very much for this comment. Indeed, fraction of non-spherical particles was also considered and used in the calculations, but it was missed in the text. The text is updated as following:
An additional criterion that was used to distinguish the aerosol type is the value of Ångström exponent (å) between wavelengths of 870 nm and 440 nm. The Ångström exponent below 0.6 is attributed to dust, between 0.8 and 1.2 to a mixed aerosol type in Dakar and Kanpur sites, above 1.6 for urban/industrial pollution in Paris, and above 1.6 for the biomass burning in the Mongu site. Average fractions of spherical particles obtained for these aerosol types were also examined. The values logically correspond to the defined aerosol models, that is: 3% for dust in Dakar; 5% for mixture of dust and biomass burning in Dakar; 21% for mixture of dust and

urban/industrial in Kanpur; 98% for urban/industrial in Paris; and 99% for biomass burning in Mongu. These values were also employed in calculations of aerosol radiative effect presented in this study.

Page 11, line 12, should be “Note that”.
Corrected.

Page 12, line 27, poor sentence structure.
Modified to the next:
Thus, for a consistent inter-comparison of radiative efficiencies calculated for different aerosol models, we choose to set all corresponding AOTs at 550 nm to unit.

Page 14, line 8, should be “than”.
Corrected.

Page 14, line 24, I suggest using “magnitude” instead of “strength”.
Corrected.

Page 15, line 13, I suggest start a new paragraph for Figure 7 to increase readability.
Corrected.

Page 15, line 18-20, the diurnal averaged radiative efficiency switches signs when the surface albedo is 0.2, not clear which mixed aerosol type you are referring here.
It is true for both mixed aerosol models. The sentence is clarified as follows:
… daily average radiative efficiency of biomass burning and both mixed aerosol models switches sign at TOA when surface albedo is brighter than about 0.15 or 0.2…

Page 20, line 27, typo “free” should be “three”.
Corrected.

Below is provided the updated version of Section 8:

8 Illustration of radiative effect calculations over Africa

In this section we illustrate feasibility of rigorous direct aerosol radiative effect calculations on large-scale using satellite observations. It is done as part of the GRASP algorithm application for POLDER/PARASOL observations. The product is of particular interest because it provides detailed aerosol characteristics, including absorption, also over bright surfaces where information about aerosol properties is rarely available. With a goal to test the computational tool and assess an observation-based aerosol radiative effect and its spatial variability, the calculations were conducted for POLDER/PARASOL observations during summer 2008 (June, July, August) over part of Africa known as one of the major sources of the desert dust. It has to be noted, however, that the GRASP algorithm is still in completion phase and that the quality of the aerosol properties retrievals is in a validation process. In this works we therefore present an inter-comparison between AOT and ω_0 retrieved by GRASP from POLDER/PARASOL and those of the conventional AERONET product. The inter-comparison is conducted using four AERONET sites with good statistic of observations and located in the area of

interest (Banizoumbou, Agoufou, IER Cinzana and DMN Maine Soroa sites). In order to increase the statistics of joint PARASOL and AERONET observations and to cover various aerosol types and surface reflectance, one year (2008) of data was analyzed. Of course, the inter-comparison at the selected sites is not fully representative for the entire area. Uncertainties can appear for cases of very low AOT, in regions with complex landscape (mountains, mixed land/water pixels) and failures of the cloud mask. Nevertheless, the conducted inter-comparison shows very encouraging correlation coefficients and small uncertainties (RMSE (Root Mean Square Error and Standard Deviation from AERONET)) both for AOT and ω_0 (see Fig. 13). The results are obtained for ±15 minutes temporal matching criteria between PARASOL and AERONET observations and for PARASOL pixels (with about 6x6 km spatial resolution) collocated to each of the selected AERONET station. In addition to comparison with AERONET, analysis of the residuals of the fit for the ensemble of the retrievals employed in this work did not indicated any major problem.

Figure 14 presents the means for three months of: i) daily average top and bottom of atmosphere net aerosol radiative effects; ii) radiative efficiencies calculated with respect to AOT at 550 nm (interpolated from nominal wavelength of POLDER); iii) AOT at 565 nm; iv) underlying surface albedo at 565 nm; and v) spectral ω_0 (presented by means of two wavelengths, 443 nm and 1020 nm). The domain averages and standard deviations of the characteristics presented in Fig. 14 are also indicated in the panels. The domain averages and standard deviations are calculated for all observations during three months of summer 2008. As shown in Fig. 14, fine spatial feature of aerosol radiative effect (at top of atmosphere in particular) can be revealed by high spatial resolution of POLDER/PARASOL. A significant amount of pixels, mostly in the northern part of Africa (e.g. central Egypt and northern part of Western Sahara), shows quite strong (up to about 10 to 20 Wm^{-2}) positive radiative effect with the corresponding radiative efficiency over 40 $Wm^{-2}\tau^{-1}$ (Fig. 14c), d)), despite that the climatological aerosol and surface models in Fig. 7 show positive radiative efficiencies of only up to 20 $Wm^{-2}\tau^{-1}$. The relatively large positive radiative effect is due to two main factors. First, it happens when the surface reflectance is higher (around 0.4 at 565 nm) and the spectral ω_0 is lower (around 0.8) compared to the limits assumed in calculations presented in Fig. 7. Evidently, the climatological aerosol and surface models represent only an average but cannot be all-inclusive of all possible variations of the properties. Second, what is more important is the non-linearity of the aerosol radiative effect as function of AOT. In fact, the AOT varies significantly in the real data (Fig. 14e)) and strong radiative efficiencies (Fig. 14c)) appear when the AOT is low, while the AOT at 550 nm was set to one in calculations of radiative efficiency presented in Fig. 7. In an attempt to illustrate and evaluate the aforementioned reasons, the aerosol models presented in Sect. 3 have been slightly modified and some supplementary calculations have been conducted. For example, the mixture of dust and biomass burning aerosol model has been assumed to be slightly more absorbing, by changing the spectral imaginary part of refractive indices k at 440/670/870/1020 nm from 0.021/0.016/0.013/0.013 to 0.025/0.016/0.016/0.016. This modification produces aerosol properties close to those retrieved for central Egypt with the spectral ω_0(440/670/870/1020 nm) of 0.80/0.81/0.81/0.81. Radiative effect and efficiency calculated for this aerosol model and for corresponding to the central Egypt surface albedo of ~0.4 at 550 nm are presented in Fig. 15 (labeled as "Absorbing mixture"). Modification of the climatological dust aerosol model by increasing k(440/670/870/1020 nm) from

0.004/0.002/0.002/0.002 to 0.008/0.006/0.006/0.006 produces aerosol properties similar to those retrieved for northern part of Western Sahara with spectral ω_0 of 0.85/0.89/0.91/0.92, for example. Results of calculations for this aerosol model and for corresponding surface albedo of ~0.35 at 550 nm are labeled in Fig. 15 as "Absorbing dust". The radiative effect calculations presented in Fig. 15 show first of all that strongly absorbing aerosols over very bright surface produce significant positive radiative effect at top of atmosphere and reproduce range of the radiative effect values obtained over central Egypt and Western Sahara. Second, Fig. 15 illustrates that because of non-linearity of the radiative effect as function of AOT, the values of the radiative efficiency are strongly dependent on AOT with which were calculated. The presented example shows variability in radiative efficiency up to 40% at top and 25% at bottom of atmosphere due to AOT ranging from 0.2 to 1. The fact implies that one should interpret the maps of radiative efficiency in Fig. 14c), d) with caution due to the spatial variation of aerosol concentration.

Noteworthy is also the obtained spectral ω_0 (Fig. 14g), h)). Although it is generally consistent with ω_0 of mineral dust (stronger absorption at 443 nm than at 1020 nm), in some cases the ω_0 appears quite low (about 0.8) at 443 and 1020 nm, which indicates presence of probably carbonaceous particles or mixed aerosol (e.g. over central Egypt). For the daily average BOA radiative effect (Fig. 14 b)) the values show quite important spatial variability and areas with strong cooling (about –60 Wm^{-2}) that generally correspond to high AOT. Overall, it can be concluded that the values obtained from POLDER/PARASOL observations are in the range of what could be expected from the theoretical climatological calculations presented in this study. The preliminary results and spatial patterns of the aerosol radiative effect thus demonstrate potential of this high advanced product of new GRASP algorithm.

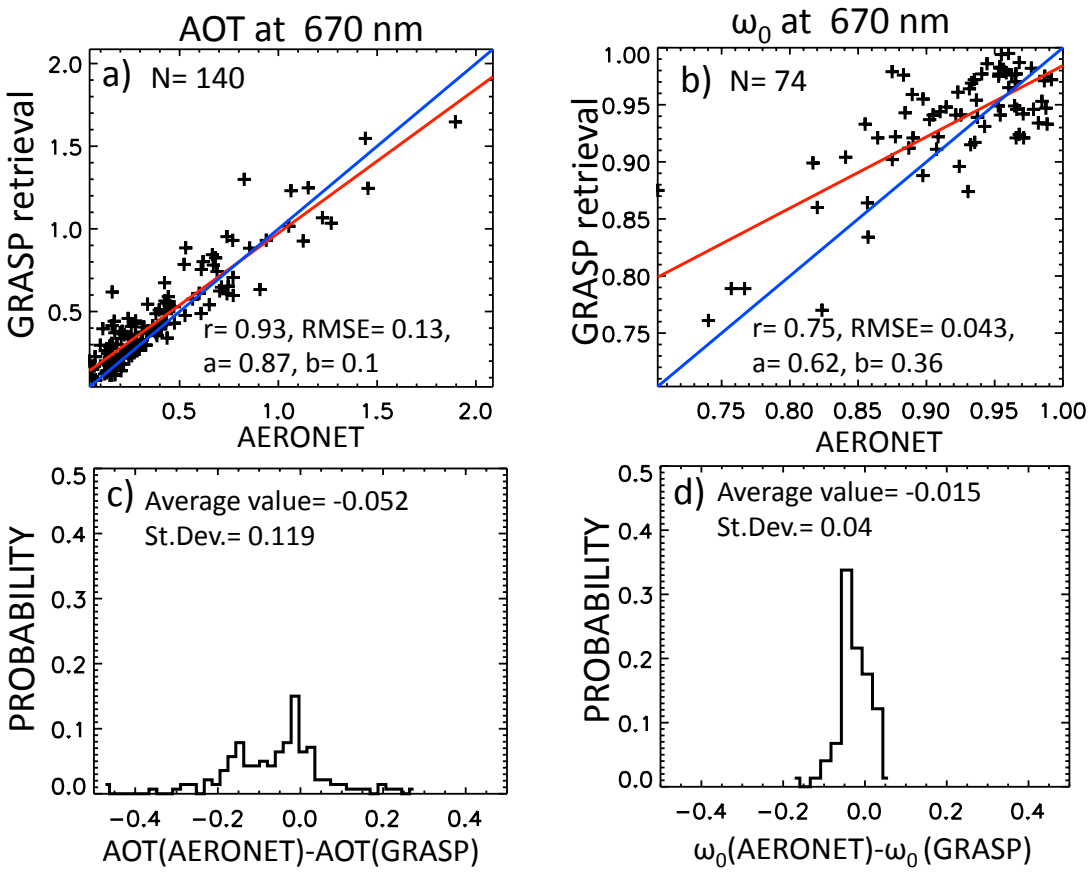

Figure 13. Inter-comparison between GRASP retrievals applied for POLDER/PARASOL observations and operational AERONET product during 2008 for ensemble of observations at four sites (Banizoumbou, Agoufou, IER Cinzana and DMN Maine Soroa). Panels a) and b) present correlations between AOT and ω_0 at 670 nm, respectively; c) and d) probability distributions of absolute differences for AOT and ω_0. The temporal threshold is 15 minutes between PARASOL and AERONET observation; the products from the ground-based measurements are compared to those from the space-borne measurements of about 6x6 km pixel that includes the site.

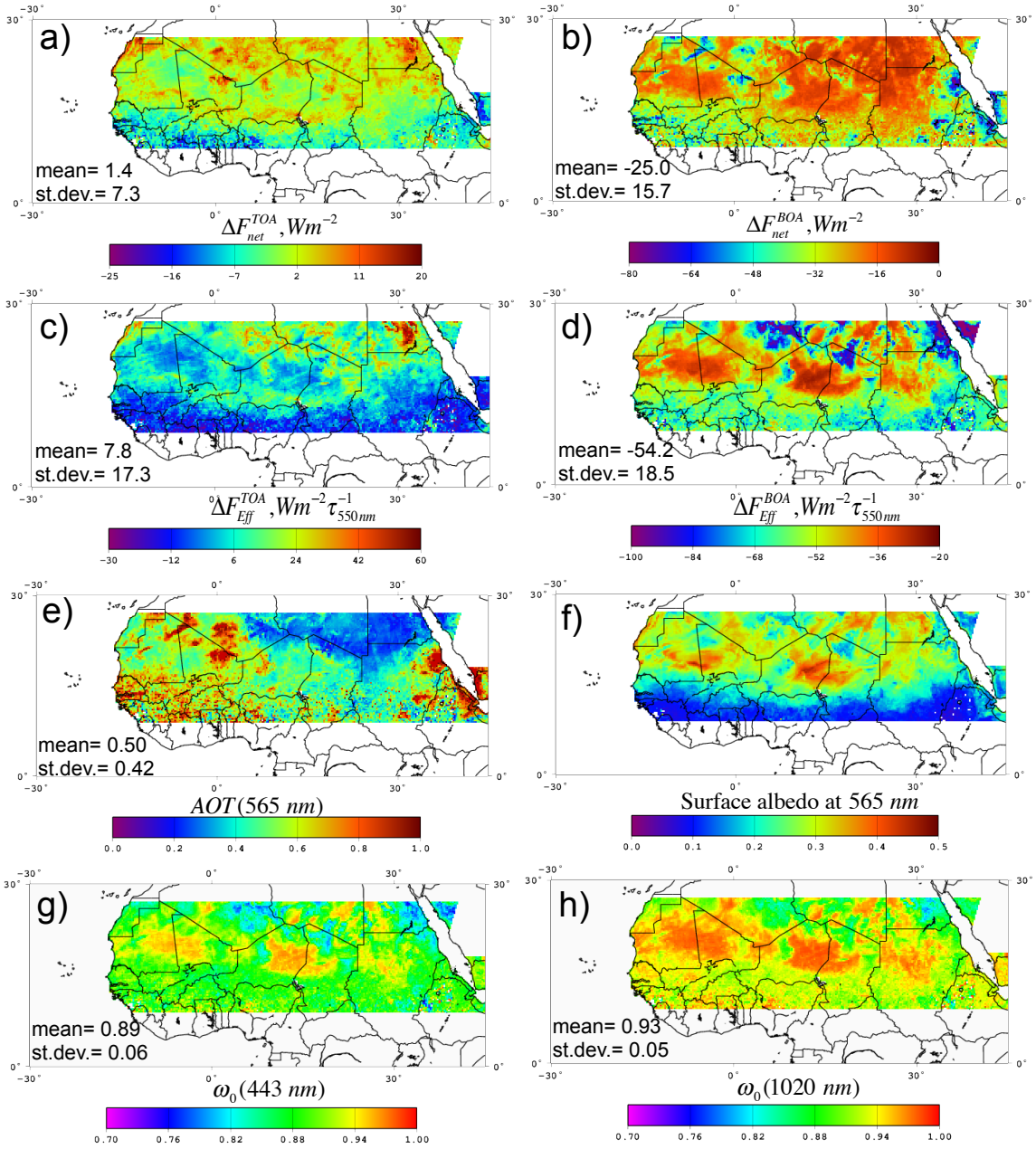

Figure 14. Three months (JJA 2008) means of a) the 24h average Top and b) 24h average Bottom Of Atmosphere (TOA and BOA) net aerosol radiative effect, c) and d) the corresponding radiative efficiencies (see Sect. 8 for the interpretation), e) AOT at 565 nm, f) underlying surface albedo at 565 nm, and g) ω_0 at 443 nm and h) at 1020 nm as retrieved and calculated by GRASP algorithm applied for POLDER/PARASOL observations. The panels also include the domain averages and corresponding standard deviations.

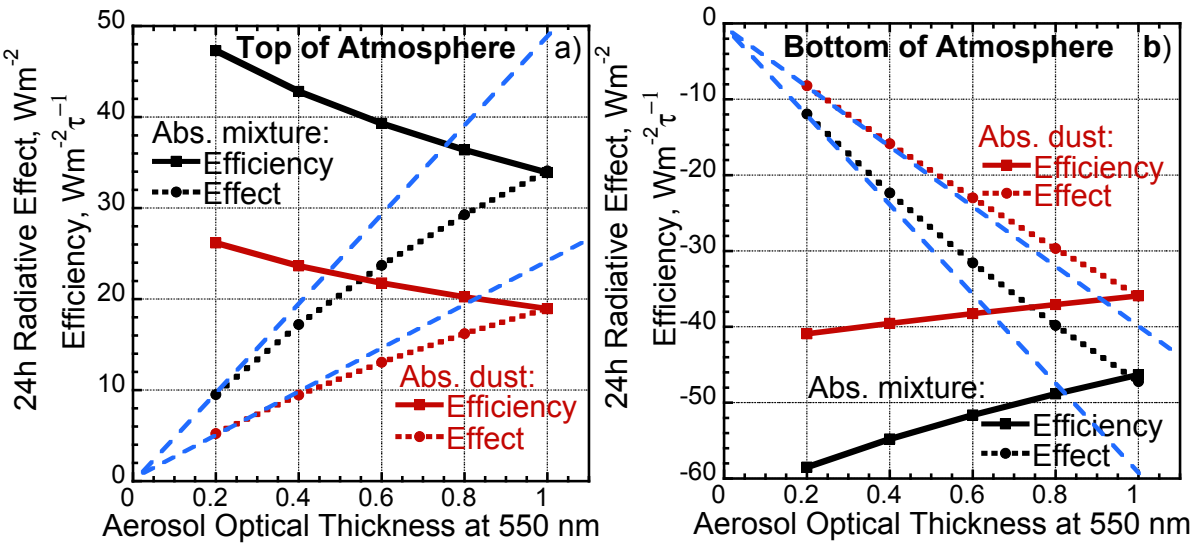

Figure 15. (dashed lines) Dependence between calculated 24h average aerosol radiative effect and AOT at 550 nm; (solid lines) 24h average aerosol radiative efficiency calculated using presented on the abscissa AOT. Black and red lines correspond respectively to "Absorbing mixture" and "Absorbing dust" aerosol models described in Sect. 8; surface albedo at 550 nm is set to 0.43 for "Absorbing mixture" and 0.34 for "Absorbing dust" scenarios; blue lines represent linear dependence between 24h average aerosol radiative effect and AOT. Panel a) is for top and b) for bottom of atmosphere.